Periodic Waveguide Structures with Long Cells

Jan Votruba, *Member, IEEE*

***Abstract*—In this paper, a class of periodic waveguide structures with stepwise constant circular cross section is analyzed by means of Hahn's method of modal field matching along transverse planes. It allows one to resolve algebraically the implicit determinant relation between the phase shift per cell and frequency and to obtain an explicit formula. Dispersion diagrams and field distributions are also calculated and plotted and convergence properties of the method are tested.**

***Index Terms*—Bandpass filters, communication channels, dispersion diagrams, periodic structures, waveguide theory.**

I. Introduction

A WAVEGUIDE with periodically stepwise constant circular cross section, i.e., the disk loaded or iris loaded waveguide, is an example of a slow-wave structure [1]. Such structures find applications in accelerator physics as accelerating or deflecting cavities and in microwave electronics as generators of microwave energy. The dimensions of periodic waveguide structures are optimized for maximum coupling to the beam of charged particles. There are also situations in which an undesirable parasitic slow-wave structure is generated. An example is a vacuum chamber of a storage ring accelerator. Such a chamber consists of long pipes inside the dipole and quadrupole magnets, and shorter sections of larger diameter between the magnets, which serve as vacuum pump-out stations. In this case, the objective is to minimize the coupling to the beam in order to suppress longitudinal instabilities due to the interaction of the beam with the excited TM_0 modes [2], [3]. This has been the motivation for studying field distributions and dispersion diagrams of such "long cell" structures. However, it seems that such structures might find utility as bandpass filters and as multichannel communication lines for transmitting signals. There are geometries that provide remarkably linear sections in dispersion curves. This means that the group velocity is constant over sizable bandwidth of frequencies in which signals propagate without dispersive distortion.

The periodic waveguide structures have been extensively investigated [4]. The most recent development in the analysis is due to Amari *et al.* [5], [6]. Their formulation is based on the coupled-integral-equation technique, which allows an arbitrary number of discontinuities per unit cell. It does not require solving a nonlinear determinant equation, and the phenomenon of relative convergence [7] is eliminated. Alternatively, the complete solution of the electromagnetic problem for these structures, i.e., solving wave equations with boundary conditions, can be obtained by dividing the structure into simple cylindrical subregions and expanding the fields into an infinite set of normal modes. The recent formulation of modal analysis is given by Esteban and Rebollar [8].

The expansion coefficients in the modal analysis are determined from an infinite system of linear homogeneous equations, which are derived by matching the solutions on the boundary between the individual subregions. The condition required for the system to have a nontrivial solution is that the determinant of the system be equal to zero. This equation is an implicit dispersion relation between the frequency and phase shift per cell of the structure. The determination of this relation is the central problem of slow-wave structures.

In this paper, it is shown that, for a special class of structures with dimensions and a frequency satisfying certain conditions, the determinant dispersion relation can be resolved algebraically and an explicit formula can be obtained for the phase shift per cell as a function of frequency. The analysis is carried out using Hahn's method of modal field matching along transverse planes. In Section II, we summarize the results of the general theory of Hahn, retaining the notation introduced in his original papers [9], [10]. The restriction to our class of structures and frequencies, defined in Section III, will allow us to derive, in Section IV, the above-mentioned dispersion relation in the form $\Phi = \Phi(f)$. Having both the frequency and phase shift per cell, we can compute, in Section V, the expansion coefficients and field distributions. In Section VI, some instructive dispersion diagrams are evaluated in a variety of structures.

II. Summary of Hahn's Theory

There is a preference in the literature to subdivide the periodic structure into cylindrical subregions and to match the fields along axial cylindrical interfaces. The disadvantage of this approach is that the phase shift per cell does not appear explicitly in the field expressions and there is no simple relation between the expansion coefficients of the cylindrical subregions. Hahn [10] investigated this and other possible ways of structure subdivisions and was able to provide a superior method for modal field matching along transverse planes. For convenience of the reader, Hahn's theory is presented below using Hahn's original notations.

We assume harmonic time variation of the field components and we use the phasor notation. Due to the cylindrical symmetry of the waveguide, we use a cylindrical coordinate system: z—coordinate along the waveguide axis, r—the radial coordinate, and ϑ—the azimuthal angle.

In the rotationally symmetric TM_0 mode, only three field components are different from zero: $E_r(r,z)$, $E_z(r,z)$, and $H_\vartheta(r,z)$. It is sufficient to consider $H_\vartheta(r,z)$ only because the other two components are determined by the relations $E_r(r,z) = jk^{-1}\partial_z H_\vartheta(r,z)$ and

Manuscript received June 18, 1999.
The author is with Votruba & Cummings, Melville, NY 11747-0236 USA.
Publisher Item Identifier S 0018-9480(00)08733-0.

0018–9480/00$10.00 © 2000 IEEE

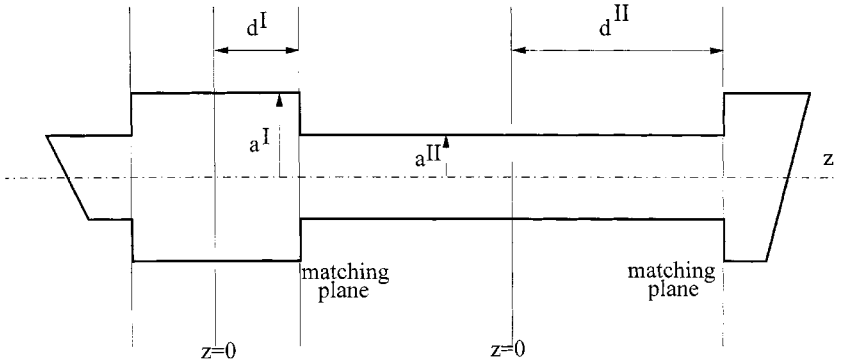

Fig. 1. Basic cell.

$E_z(r,z) = -j(kr)^{-1}\partial_r(rH_\vartheta(r,z))$, where $k = 2\pi f/c$. In periodic structures, the entire $H_\vartheta(r,z)$ field component, as well as all other field components, phase shift by $\exp(-j\beta_0 L)$ in moving from z to $z+L$, where L is the period of the structure. The quantity β_0 is the fundamental reference propagation constant and the phase $\beta_0 L = \Phi$ is called the phase shift per cell.

Fig. 1 schematically shows the basic cell of the structure, together with dimensions and matching planes. In accordance with [9] and [10], we divide the basic cell into subregion I with the larger radius a^{I} and length $2d^{\mathrm{I}}$, and subregion II with the smaller radius a^{II} and length $2d^{\mathrm{II}}$.

The azimuthal magnetic component of the rotationally symmetric transversal magnetic TM_0 mode in subregion I is expanded into normal modes

$$H_\vartheta^{\mathrm{I}}(r,z) = \sum_{m=1}^{\infty}\left(-ju_m^{\mathrm{I}}\frac{\sin k_{zm}^{\mathrm{I}}z}{\cos k_{zm}^{\mathrm{I}}d^{\mathrm{I}}} + i_m^{\mathrm{I}}\frac{\cos k_{zm}^{\mathrm{I}}z}{\sin k_{zm}^{\mathrm{I}}d^{\mathrm{I}}}\right)\cdot Y_m^{\mathrm{I}}\rho(k_{rm}^{\mathrm{I}}r) \quad (1)$$

where the origin $z=0$ is put in the center of subregion I. Similarly, in subregion II

$$H_\vartheta^{\mathrm{II}}(r,z) = \exp\left(-\frac{j}{2}\Phi\right)\sum_{m=1}^{\infty}\left(-ju_m^{\mathrm{II}}\frac{\sin k_{zm}^{\mathrm{II}}z}{\cos k_{zm}^{\mathrm{II}}d^{\mathrm{II}}} + i_m^{\mathrm{II}}\frac{\cos k_m^{\mathrm{II}}z}{\sin k_m^{\mathrm{II}}d^{\mathrm{II}}}\right)\cdot Y_m^{\mathrm{II}}\rho(k_{rm}^{\mathrm{II}}r). \quad (2)$$

The origin is now put in the center of subregion II. The orthonormal radial basic functions ρ are

$$\rho(k_{rm}^i r) = \frac{J_1(k_{rm}^i r)}{\pi^{1/2}a^i J_1(j_{0m})}, \qquad i = \mathrm{I},\mathrm{II}. \quad (3)$$

In (1)–(3)

$$k = 2\pi f/c \quad (4)$$
$$k_{rm}^i = j_{0m}/a^i \quad (5)$$
$$k_{zm}^i = (k^2 - (k_{rm}^i)^2)^{1/2} \quad (6)$$
$$Y_m^i = k/k_{zm}^i \quad (7)$$

f is the frequency, c is the speed of light, and j_{0m} are zeros of the Bessel function J_0. The expansion coefficients u_m^{II} and i_m^{II} are solutions of the system of homogeneous linear equations

$$\begin{pmatrix} M_{11} & M_{12} \\ -M_{12} & M_{22}\end{pmatrix}\begin{pmatrix} u^{\mathrm{II}} \\ i^{\mathrm{II}}\end{pmatrix} = \begin{pmatrix} 0 \\ 0\end{pmatrix} \quad (8)$$

with the block matrices

$$M_{11} = \tilde{A}Y^{\mathrm{I}}S^{2\mathrm{I}-1}A\cdot\cos\Phi - \tilde{A}Y^{\mathrm{I}}T^{2\mathrm{I}-1}A + Y^{\mathrm{II}}T^{\mathrm{II}} \quad (9)$$
$$M_{22} = \tilde{A}Y^{\mathrm{I}}S^{2\mathrm{I}-1}A\cdot\cos\Phi + \tilde{A}Y^{\mathrm{I}}T^{2\mathrm{I}-1}A + Y^{\mathrm{II}}T^{\mathrm{II}-1} \quad (10)$$
$$M_{12} = \tilde{A}Y^{\mathrm{I}}S^{2\mathrm{I}-1}A\cdot\sin\Phi. \quad (11)$$

Here, Y^i, $S^{2\mathrm{I}-1}$, $T^{2\mathrm{I}-1}$, T^{II}, and $T^{\mathrm{II}-1}$ are the following diagonal matrices: $Y^i = Y_m^i\delta_{mn}$, $S^{2\mathrm{I}-1} = S_m^{2\mathrm{I}-1}\delta_{mn}$, $T^{2\mathrm{I}-1} = T_m^{2\mathrm{I}-1}\delta_{mn}$, $T^{\mathrm{II}} = T_m^{\mathrm{II}}\delta_{mn}$, and $T^{\mathrm{II}-1} = T_m^{\mathrm{II}-1}\delta_{mn}$, where $S_m^{2\mathrm{I}-1} = 1/\sin 2k_{zm}^{\mathrm{I}}d^{\mathrm{I}}$, $T_m^{2\mathrm{I}-1} = \cot 2k_{zm}^{\mathrm{I}}d^{\mathrm{I}}$, $T_m^{\mathrm{II}} = \tan k_{zm}^{\mathrm{II}}d^{\mathrm{II}}$, and $T_m^{\mathrm{II}-1} = \cot k_{zm}^{\mathrm{II}}d^{\mathrm{II}}$. The matching matrix A has the elements

$$A_{mn} = \frac{2x^2 j_{om}J_0(xj_{0m})}{(j_{0n}^2 - x^2 j_{0m}^2)J_1(j_{0m})}, \qquad \tilde{A}_{mn} = A_{nm} \quad (12)$$

where

$$x = a^{\mathrm{II}}/a^{\mathrm{I}} < 1. \quad (13)$$

The phase shift per cell Φ is related to the frequency f by the equation

$$\det M = 0 \quad (14)$$

where the symbol $\det M$ means the determinant of the matrix

$$M = \begin{pmatrix} M_{11} & M_{12} \\ -M_{12} & M_{22}\end{pmatrix}. \quad (15)$$

The coefficients u_m^{I} and i_m^{I} are determined by the matrix equation

$$\begin{pmatrix} u^{\mathrm{I}} \\ i^{\mathrm{I}}\end{pmatrix} = \begin{pmatrix} A\cdot\cos\frac{1}{2}\Phi & A\cdot\sin\frac{1}{2}\Phi \\ A\cdot\sin\frac{1}{2}\Phi & -A\cdot\cos\frac{1}{2}\Phi\end{pmatrix}\begin{pmatrix} u^{\mathrm{II}} \\ i^{\mathrm{II}}\end{pmatrix}. \quad (16)$$

Thus, for a given geometry and for a given frequency, the $H_\vartheta(r,z)$ component of the TM_0 mode propagating through the

basic cell is completely described. The remaining components $E_r(r,z)$ and $E_z(r,z)$ are given by the relations $E_r(r,z) = jk^{-1}\partial_z H_\vartheta(r,z)$ and $E_z(r,z) = -j(kr)^{-1}\partial_r(rH_\vartheta(r,z))$. If one denumerates the basic cell by the index $K = 0$ then, by applying the Floquet theorem, the field in the Kth cell of the structure is equal to the field in the basic cell times the phase factor $\exp(-jK\Phi)$.

III. Specification of the Waveguide

For fixed quantity k, i.e., for a given frequency, the quantity k_{zm}^i becomes imaginary starting from a certain value of the index m. Thus, as seen from (1) and (2), there are two kinds of modes: The first, m propagating modes described by sines and cosines, and the remaining infinitely many evanescent modes, generated at the structure discontinuities, described by hyperbolic sines and hyperbolic cosines. In this paper we describe in detail the field in the frequency interval $cj_{01}/2\pi a^{\mathrm{I}} < f < cj_{02}/2\pi a^{\mathrm{I}}$. For this situation, series (1) can be rewritten in the form

$$H_\vartheta^{\mathrm{I}}(r,z) = \left(-ju_1^{\mathrm{I}}\frac{\sin k_{z1}^{\mathrm{I}}z}{\cos k_{z1}^{\mathrm{I}}d^{\mathrm{I}}} + i_1^{\mathrm{I}}\frac{\cos k_{z1}^{\mathrm{I}}z}{\sin k_{z1}^{i}d^{\mathrm{I}}}\right)Y_1^{\mathrm{I}}\rho(k_{r1}^{\mathrm{I}}r) + \sum_{m=2}^{\infty}\left(-j\frac{z}{|z|}u_m^{\mathrm{I}} - i_m^{\mathrm{I}}\right) \cdot \exp\Big(-\kappa_{zm}^{\mathrm{I}}\big(d^{\mathrm{I}} - |z|\big)\Big)\eta_m^{\mathrm{I}}\rho(k_{rm}^{\mathrm{I}}r) \tag{17}$$

where

$$\kappa_{zm}^{\mathrm{I}} = \big((k_{rm}^{\mathrm{I}})^2 - k^2\big)^{1/2} \quad \eta_m^{\mathrm{I}} = k/\kappa_{zm}^{\mathrm{I}}, \qquad m \geq 2. \tag{18}$$

In other words, we still need infinitely many normal modes to describe the field, but only the first one has a constant amplitude in subregion I. It will be shown in Section IV that of special interest is the case in which the quantity $1/\sinh 2\kappa_{zm}^{\mathrm{I}}d^{\mathrm{I}}$ is negligibly small for $m \geq 2$. In this case, determinant relation (14) between the phase shift per cell Φ and the frequency f can be resolved algebraically. Let us, for instance, consider $1/\sinh 2\kappa_{zm}^{\mathrm{I}}d^{\mathrm{I}}$ to be negligibly small with respect to unity and, as such, replaced by zeros in subsequent expressions, if

$$2\kappa_{zm}^{\mathrm{I}}d^{\mathrm{I}} > \varepsilon, \qquad \text{for } m \geq 2. \tag{19}$$

The number ε can be chosen by what we want to consider negligible in numerical calculations. If, for instance, $\varepsilon = 10$, then

$$1/\sinh(2\kappa_{zm}^{\mathrm{I}}d^{\mathrm{I}}) < 10^{-4} \ll 1, \qquad \text{for } m \geq 2. \tag{20}$$

Using (4), (5), (18), and (19), we find

$$d^{\mathrm{I}} > \frac{\varepsilon c}{4\pi}\left[\left(\frac{cj_{02}}{2\pi a^{\mathrm{I}}}\right)^2 - f^2\right]^{-1/2}, \qquad f < cj_{02}/2\pi a^{\mathrm{I}}$$

which shows that the length of subregion I is limited from below. This clarifies what is meant by a "long cell structure." On the other hand, for a given d^{I} and $f > (cj_{01}/2\pi a^{\mathrm{I}})$, we find from the above formula

$$\frac{cj_{01}}{2\pi a^{\mathrm{I}}} < f < \left[\left(\frac{cj_{02}}{2\pi a^{\mathrm{I}}}\right)^2 - \left(\frac{\varepsilon c}{4\pi d^{\mathrm{I}}}\right)^2\right]^{1/2} = f_{\max}. \tag{21}$$

Let us introduce the notation $f_k^i = cj_{0k}/2\pi a^i$, $k = 1,2,\ldots, i = \mathrm{I},\mathrm{II}$ for the cutoff frequencies. Then, as stated above, $f_1^{\mathrm{I}} < f < f_{\max}$. Due to (13), we always have $f_1^{\mathrm{I}} < f_1^{\mathrm{II}}$. Depending on the value of the ratio $x = (a^{\mathrm{II}}/a^{\mathrm{I}})$, two cases can be considered: $f_1^{\mathrm{II}} > f_{\max}$ and $f_1^{\mathrm{II}} < f_{\max}$.

1) We call the structure "deep" if $f_1^{\mathrm{II}} > f_{\max}$, from which we find

$$\frac{a^{\mathrm{II}}}{a^{\mathrm{I}}} < \left[\left(\frac{j_{01}}{j_{02}}\right)^2 + \varepsilon^2\left(\frac{a^{\mathrm{II}}}{d^{\mathrm{I}}j_{02}}\right)^2\right]^{1/2}. \tag{22}$$

In this case, $f < [(f_2^{\mathrm{I}})^2 - (\varepsilon c/4\pi d^{\mathrm{I}})^2]^{1/2} < f_1^{\mathrm{II}}$, and no mode can propagate through subregion II without attenuation. For this situation, (2) can be written in the form

$$H_\vartheta^{\mathrm{II}}(r,z) = \exp\left(-\frac{j}{2}\Phi\right)\sum_{m=1}^{\infty}\left(-j\frac{z}{|z|}u_m^{\mathrm{II}} + i_m^{\mathrm{II}}\right) \cdot \exp\big(-\kappa_{zm}^{\mathrm{II}}(d^{\mathrm{II}} - |z|)\big)\eta_m^{\mathrm{II}}\rho(k_{rm}^{\mathrm{II}}r) \tag{23}$$

where

$$\kappa_{zm}^{\mathrm{II}} = \big((k_{rm}^{\mathrm{II}})^2 - k^2\big)^{1/2} \quad \text{and} \quad \eta_m^{\mathrm{II}} = k/\kappa_{zm}^{\mathrm{II}}.$$

To assure the integrity of the structure (so that it does not break down into independent cavities—subregions I), we introduce the condition

$$2\kappa_{z1}^{\mathrm{II}}d^{\mathrm{II}} < \varepsilon.$$

Using (4) and (5), we find

$$d^{\mathrm{II}} < \frac{\varepsilon c}{4\pi}\left[\left(\frac{cj_{01}}{a^{\mathrm{II}}}\right)^2 - f^2\right]^{-1/2}$$

which shows that the smaller the radius a^{II} of the opening in the "iris," the thinner the "iris," must be, i.e., the shorter subregion II must be.

2) The structure is "shallow" if $f_1^{\mathrm{II}} < f_{\max}$. Then

$$\frac{a^{\mathrm{II}}}{a^{\mathrm{I}}} > \left[\left(\frac{j_{01}}{j_{02}}\right)^2 + \varepsilon^2\left(\frac{a^{\mathrm{II}}}{d^{\mathrm{I}}j_{02}}\right)^2\right]^{1/2}. \tag{24}$$

In this case, a bandwidth of frequencies

$$f_1^{\mathrm{II}} < f < \left[(f_2^{\mathrm{I}})^2 - \left(\frac{\varepsilon c}{4\pi d^{\mathrm{I}}}\right)^2\right]^{1/2} \tag{25}$$

can be available in which the first mode in subregion II can propagate freely. We can write

$$H_\vartheta^{\mathrm{II}}(r,z) = \exp\left(-\frac{j}{2}\Phi\right)\left[\left(-ju_1^{\mathrm{II}}\frac{\sin k_{z1}^{\mathrm{II}}z}{\cos k_{z1}^{\mathrm{II}}d^{\mathrm{II}}} + i_1^{\mathrm{II}}\frac{\cos k_{z1}^{\mathrm{II}}z}{\sin k_{z1}^{\mathrm{II}}d^{\mathrm{II}}}\right)Y_1^{\mathrm{II}}\rho(k_{r1}^{\mathrm{II}}r) + \sum_{m=2}^{\infty}\left(-j\frac{z}{|z|}u_m^{\mathrm{II}} - i_m^{\mathrm{II}}\right) \cdot \exp\big(-\kappa_{zm}^{\mathrm{II}}(d^{\mathrm{II}}-|z|)\big)\eta_m^{\mathrm{II}}\rho(k_{rm}^{\mathrm{II}}r)\right]. \quad (26)$$

IV. Dispersion Formula

The determination of the phase shift per cell Φ as a function of frequency is the central problem of periodic structures. The solution usually consists in trying to satisfy (14) by trial and error, and it can be quite tedious if one attempts to find many points to draw dispersion curves. In this section, due to the restricting conditions defined in Section III, we will be able to actually resolve implicit relation (14) and to derive an explicit formula for the phase shift per cell as a function of frequency.

For computational purposes, it is necessary to truncate the infinite series and infinite matrices introduced in Section II. The value of the phase shift per cell will be influenced by our choice of the number M of terms in series (17) and the number N of terms in series (23) or (26). We, therefore, introduce new notation $\Phi_{M,N}$. How much the value of $\Phi_{M,N}$ will differ from the value of the unknown asymptotic Φ is related to the convergence properties of the method, which will be discussed in Sections V and VI.

While matching matrix (12) is rectangular, with M rows and N columns, block matrices (9)–(11) have dimensions $N \times N$ and matrix (15) has dimensions $2N \times 2N$.

As the first step, let us return to the diagonal matrix $S^{2\mathrm{I}-1}$ introduced in Section II. According to Section III, we have $S_1^{2\mathrm{I}-1} = 1/\sin 2k_{z1}^{\mathrm{I}}d^{\mathrm{I}}$, but $S_m^{2\mathrm{I}-1} = -j\sinh 2\kappa_{zm}^{\mathrm{I}}d^{\mathrm{I}}$ for $m \geq 2$. Due to (20), the matrix elements $S_m^{2\mathrm{I}-1}$ for $m \geq 2$ are negligible. The resulting $N \times N$ matrix $S^{2\mathrm{I}-1}$ has only one element different from zero: the element $S_1^{2\mathrm{I}-1}$. This simplifies greatly the $N \times N$ matrix $\tilde{A}Y^{\mathrm{I}}S^{2\mathrm{I}-1}A$ contained in (9)–(11). It has the form $(\tilde{A}Y^{\mathrm{I}}S^{2\mathrm{I}-1}A)_{mn} = Y_1^{\mathrm{I}}S_1^{2\mathrm{I}-1}A_{1m}A_{1n}$. Now, using basic procedures, $2(N^2+1)$ vanishing elements can be produced in the $2N \times 2N$ matrix (15). Namely, we multiply the first row by the factor A_{12}/A_{11} and we subtract it from the second row. We then multiply the first row by the factor A_{13}/A_{11} and we subtract it from the third row. We continue this procedure up to the Nth row. Similarly, we multiply the $(N+1)$th row sequentially by factors A_{1n}/A_{11} and we subtract it correspondingly from the $(N+n)$th row, i.e., $n = 2, \ldots, N$. We apply the same procedure to the columns. As a result, all elements in the block matrices M_{12} and $-M_{12}$ become zero, except the matrix elements $(M_{12})_{11}$ and $(-M_{12})_{11}$. The same happens to the matrices $\tilde{A}Y^{\mathrm{I}}S^{2\mathrm{I}-1}A \cdot \cos\Phi_{M,N}$, which are parts of the block matrices M_{11} and M_{22}. The resulting matrix M now contains only two elements with $\sin\Phi_{M,N}$ and two elements with $\cos\Phi_{M,N}$. We rearrange the rows and columns in such a way that the elements with $\sin\Phi_{M,N}$ and $\cos\Phi_{M,N}$ form a 2×2 submatrix in the upper left-hand-side corner of the matrix M. Now applying a similar procedure to that described above, we still produce $4(N-2)$ more zeros in the first and second rows and in the first and the second columns: $N-2$ zeros in each. It is then feasible to partially develop the determinant $\det M$ and to obtain from (14) the following dispersion formula:

$$2\pi l \pm \Phi_{M,N} = \arccos\left(-\frac{s^2+pq}{s(p+q)}\right), \quad l = \pm 1, \pm 2, \ldots, \pm\infty. \quad (27)$$

Here

$$\begin{aligned}
s &= Y_1^{\mathrm{I}}S_1^{2\mathrm{I}-1}A_1^2\\
p &= \alpha_{11} - \alpha_{12}^2 d_\alpha/D_\alpha\\
q &= \beta_{11} - \beta_{12}^2 d_\beta/D_\beta\\
D_\alpha &= \det(\alpha_{mn})\\
D_\beta &= \det(\beta_{mn}), \qquad m,n = 2,\ldots,N\\
d_\alpha &= \det\Big(\alpha_{mn} - \big((\alpha_{1m}\alpha_{2n} + \alpha_{2m}\alpha_{1n})\alpha_{12} - \alpha_{1m}\alpha_{1n}\alpha_{22}/\alpha_{12}^2\big)\Big), \quad m,n = 3,\ldots,N\\
d_\beta &= \det\Big(\beta_{mn} - \big((\beta_{1m}\beta_{2n} + \beta_{2m}\beta_{1n})\beta_{12} - \beta_{1m}\beta_{1n}\beta_{22}/\beta_{12}^2\big)\Big), \quad m,n = 3,\ldots,N\\
\alpha_{11} &= -Y_1^{\mathrm{I}}T_1^{2\mathrm{I}-1}A_{11}^2 + F_1\\
\beta_{11} &= Y_1^{\mathrm{I}}T_1^{2\mathrm{I}-1}A_{11}^2 - F_2\\
\alpha_{1n} &= a_{1n} - F_1A_{1n}/A_{11}\\
\beta_{1n} &= -a_{1n} + F_2A_{1n}/A_{11}, \qquad n = 2,\ldots,N\\
\alpha_{mn} &= a_{mn} - (X_{mn} - A_{1m}A_{1n}F_1)/A_{11}^2 + \delta_{mn}\eta_n^{\mathrm{II}} \cdot \tanh\kappa_{zn}^{\mathrm{II}}d^{\mathrm{II}}, \qquad m,n = 2,\ldots,N\\
\beta_{mn} &= -a_{mn} + (X_{mn} - A_{1m}A_{1n}F_2)/A_{11}^2 - \delta_{mn}\eta_1^{\mathrm{II}} \cdot \coth\kappa_{z1}^{\mathrm{II}}d^{\mathrm{II}}, \qquad m,n = 2,\ldots,N\\
a_{mn} &= \sum_{k=2}^{M}\eta_k^{\mathrm{I}}A_{km}A_{kn}, \qquad m,n = 1,\ldots,N,\\
X_{mn} &= A_{11}(A_{1m}a_{1n} + a_{1m}A_{1n}), \qquad m,n = 2,\ldots,N.
\end{aligned}$$

If $f \geq cj_{01}/2\pi a^{\mathrm{II}}$, then $F_1 = a_{11} + Y_1^{\mathrm{II}}T_1^{\mathrm{II}}$, $F_2 = a_{11} - Y_1^{\mathrm{II}}T_1^{\mathrm{II}-1}$.

If $f < cj_{01}/2\pi a^{\mathrm{II}}$, then $F_1 = a_{11} + \eta_1^{\mathrm{II}}\tanh\kappa_{z1}^{\mathrm{II}}d^{\mathrm{II}}$, $F_2 = a_{11} + \eta_1^{\mathrm{II}}\coth\kappa_{z1}^{\mathrm{II}}d^{\mathrm{II}}$.

The advantage of (27) for calculating dispersion diagrams is as follows. To find the phase shift per cell for a fixed frequency without (27) and only by means of (14), one first has to insert a trial phase Φ_0 into the matrix M and calculate the whole $2N \times 2N$ determinant. Then, repeating the calculations several times,

one tries to satisfy (14) by iteration. On the other hand, having (27), one calculates only two $(N-1)\times(N-1)$ determinants, D_α and D_β, and two $(N-2)\times(N-2)$ determinants, d_α and d_β, and there are no iterations. Moreover, various symmetry relations among the introduced quantities can be exploited in the computer code.

The dispersion diagrams can be constructed by means of (27) using a FORTRAN DO-loop with the frequency as an independent variable changed in small regular steps. The DO-loop contains the following test. If in (27) the quantity $|(s^2+pq)/(s(p+q))| > 1$, then go to the next step. This is the case of a stopband frequency region. If $|(s^2+pq)/(s(p+q))| \le 1$, then write down the frequency f and the resulting phase shift per cell $\Phi_{M,N}$, and go to the next step. An automatic regulation of the frequency step size makes the step in the stopbands ten or more times bigger then in the passbands in order to save computer time.

V. Field Distributions and Convergence Considerations

Having the phase shift per cell $\Phi_{M,N}$ available, we can insert it back into (15). Homogeneous system (8) of the linear equations for the unknown expansion coefficients u_m^{II} and i_m^{II} now has a nontrivial solution because (14) is satisfied. In order to solve this system, we omit one of its equations, i.e., the last one for instance. Setting $i_N = 1$, we then obtain a system of $2N-1$ inhomogeneous linear equations for $2N-1$ unknown coefficients u_m^{II}, $m = 1,\ldots,N$, and i_m^{II}, $m = 1,\ldots,N-1$. This system can be solved by a computer routine. The coefficients u_m^{I} and i_m^{I} follow from (16). The field distributions are now fully determined for a given frequency and given dimensions of the waveguide structure.

The truncation of series (23) or (26), i.e., their abrupt termination, causes a mismatch error when approaching the transverse matching plane between subregions I and II. However, if we limit the range of the variable z to the interval $-(d^{\mathrm{II}}-\delta^{\mathrm{II}}) \le z \le (d^{\mathrm{II}}-\delta^{\mathrm{II}})$, where δ^{II} is the thickness of a thin cutoff slab along the matching plane, the truncation error can be suppressed. Namely, at the distance $|z| \le d^{\mathrm{II}}-\delta^{\mathrm{II}}$, the evanescent modes, characterized by the exponentials $\exp(-\kappa_{zm}^{\mathrm{II}}(d^{\mathrm{II}}-|z|))$, decay rapidly with increasing index m. Starting at certain $m = N$, the contribution from the remainder of the infinite series (23) or (26) will be practically equal to zero at $|z| \le d^{\mathrm{II}}-\delta^{\mathrm{II}}$. For instance, if $\exp(-\kappa_{zN}^{\mathrm{II}}\delta^{\mathrm{II}}) \le \Delta = 0.005 \ll 1$, then the contribution from the last Nth term at the boundary of the "matching gap" will be 0.005 times smaller then its value at the matching plane and, as such, completely negligible. In other words, finite series are sufficient for a practically exact description of the field in this restricted area.

The same reasoning can be applied to subregion I characterized by series (17). For the symmetrical cutoff $\delta^{\mathrm{I}} = \delta^{\mathrm{II}} = \delta$ and for the same percentage of the last evanescent mode decay, we have $\Delta \ge \exp(-\kappa_{zN}^{\mathrm{II}}\delta) \simeq \exp(-\kappa_{zM}^{\mathrm{I}}\delta)$. Using (5) and (18), we see that $a^{\mathrm{II}}/a^{\mathrm{I}} \simeq j_{0N}/j_{0M} \simeq N/M$ with the result

$$a^{\mathrm{I}} : a^{\mathrm{II}} \simeq M : N. \tag{28}$$

Once the optimum ratio $M : N$ has been determined for a given N, one can address the question of precision of the method by increasing the number N keeping the ratio $M : N$ unchanged.

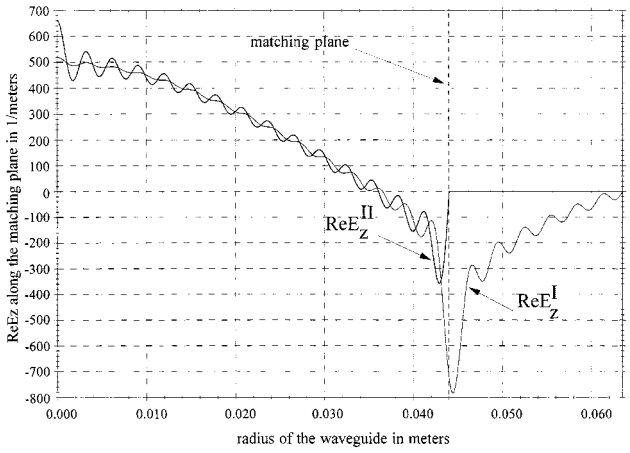

(a)

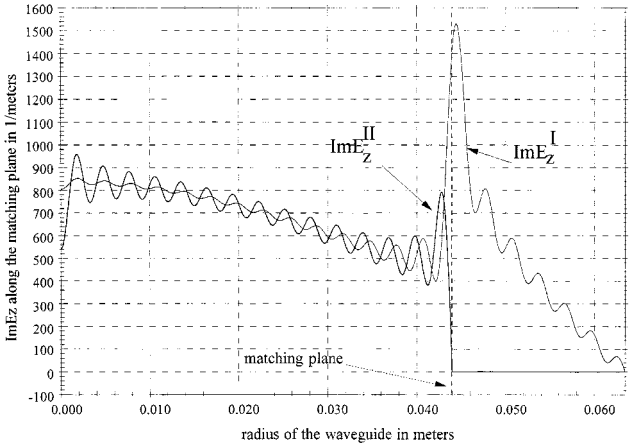

(b)

Fig. 2. (a) Real part of E_z along the matching plane. (b) Imaginary part of E_z along the matching plane.

An example of a long cell periodic waveguide structure with a stepwise constant circular cross section is the vacuum chamber of a storage ring accelerator. A realistic vacuum chamber consists of pieces of pipes in dipole and quadrupole magnets of different lengths of the same diameter, which are connected by pump-out cavities of a larger diameter between the magnets. There are also beam intersection regions. For simplicity, we consider an infinite chain of cells, shown in Fig. 1, with the dimensions in meters: $a^{\mathrm{I}} = 0.0635$ m, $d^{\mathrm{I}} = 0.165$ m, $a^{\mathrm{II}} = 0.044$ m, $d^{\mathrm{II}} = 2.75$ m. Keeping $\varepsilon = 10$, we find from (24) that this structure is "shallow"

$$a^{\mathrm{II}}/a^{\mathrm{I}} = 0.6929 > \left[\left(\frac{j_{01}}{j_{02}}\right)^2 + \varepsilon^2\left(\frac{a^{\mathrm{II}}}{d^{\mathrm{I}}j_{02}}\right)^2\right]^{1/2} = 0.65051$$

and (25) yields the available bandwidth of allowed frequencies 2607.76 MHz $< f <$ 3887.59 MHz. For the frequency $f = 2622.06$ MHz and $M = 43$, $N = 30$, for instance, (27) gives $\Phi_{43,30} = 1.57296$ rad $\simeq \pi/2$. The choice $M = 43$, $N = 30$ approximately satisfies (28). Fig. 2(a) and (b) shows the components $\mathrm{Re}E_z^{\mathrm{I}}(d^{\mathrm{I}},r)$, $\mathrm{Re}E_z^{\mathrm{II}}(-d^{\mathrm{II}},r)$ and $\mathrm{Im}E_z^{\mathrm{I}}(d^{\mathrm{I}},r)$, $\mathrm{Im}E_z^{\mathrm{II}}(-d^{\mathrm{II}},r)$ in the matching plane along

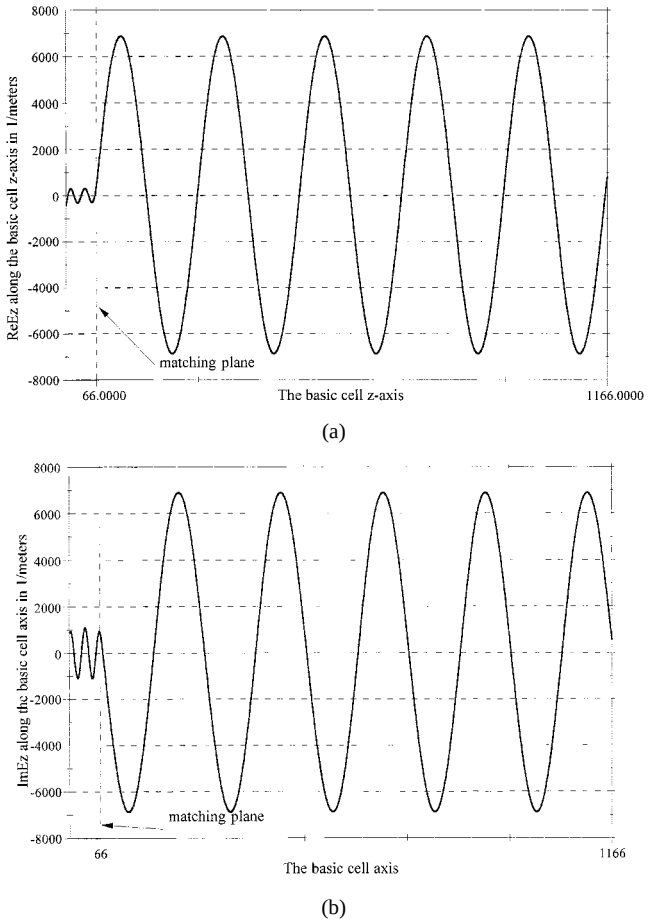

Fig. 3. (a) Real part of E_z along the basic cell axis. (b) Imaginary part of E_z along the basic cell axis.

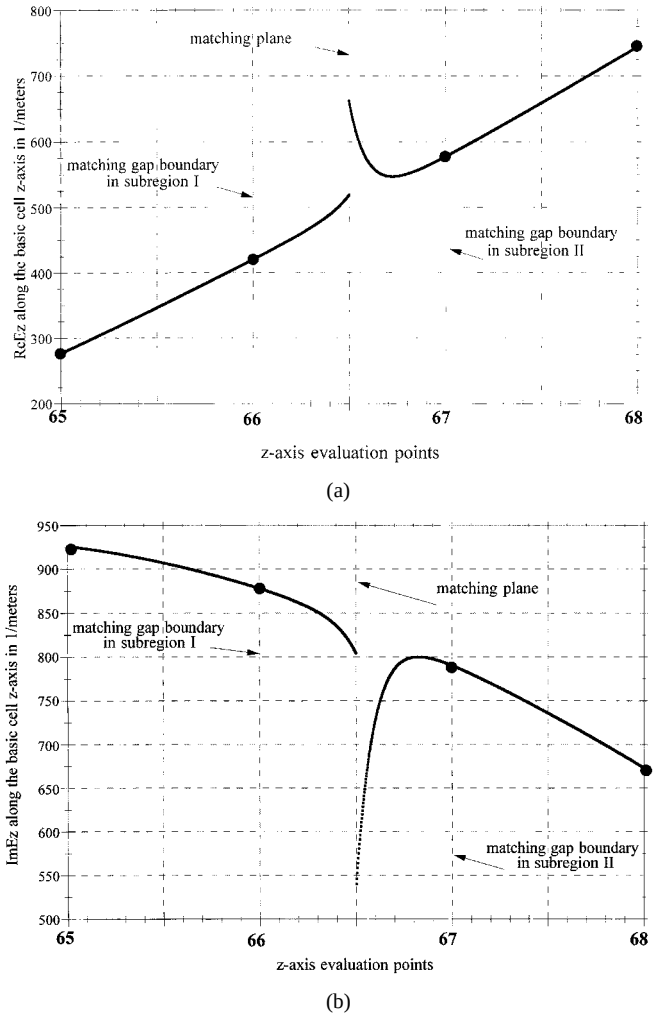

Fig. 4. (a) Real part of E_z along the basic cell axis. (b) Imaginary part of E_z along the basic cell axis. (Detail of the residual dicontinuity at the matching plane.)

the radius of the basic cell (in Fig. 1). The areas between the interlacing Gibbs oscillations are smaller in the middle of the interval $0 \leq r \leq a^{\mathrm{II}}$ and bigger near the center $r = 0$. The spike near the discontinuity at $r = a^{\mathrm{II}}$ becomes narrower and higher with increasing M and N. The number of half-wavelengths of the oscillations coincides with numbers M and N.

Taking again $\Delta = 0.005$, we can cut off a slab of the thickness $\delta = -(\ln\Delta/\kappa^{\mathrm{I}}_{z43}) \simeq -(\ln\Delta/\kappa^{\mathrm{II}}_{z30}) = 0.0025$ m on each side of the matching plane, 0.0025 m in subregion I and 0.0025 m in subregion II, i.e., $2\delta = 0.005$ m in total. The total length of the basic cell is $2d^{\mathrm{I}} + 2d^{\mathrm{II}} = 0.330m + 5.500$ m. Evaluating the field at a discrete set of points 0.005 m apart, we have 66 points in subregion I and 1100 points in subregion II; point 66 lying in the matching plane. It is advantageous to shift the whole pattern to the left by 1/2 of the step, i.e., by 0.0025 m. The matching gap 2δ will then be positioned between points 66 and 67. In this way, the residual discontinuities due to the truncation of the infinite series (17) and (26) will be made invisible. Fig. 3(a) and (b) shows the complete real and imaginary parts $\mathrm{Re}\, E_z(r,z)$ and $\mathrm{Im}\, E_z(r,z)$ in the basic cell along the z-axis ($r = 0$). Fig. 4(a) and (b) shows the region 2δ between points 66 and 67 zoomed, revealing the residual discontinuities in detail. They do not influence evaluation points in Fig. 3(a) and in (b) and they are, therefore, invisible. As a result, the actual field distribution is determined practically exactly at a finite set of discrete points, provided the value of $\Phi_{M,N}$ reached the asymptotic value of Φ. It will be demonstrated in the following section that, for the above example with $\Phi_{43,30}$, this is actually the case.

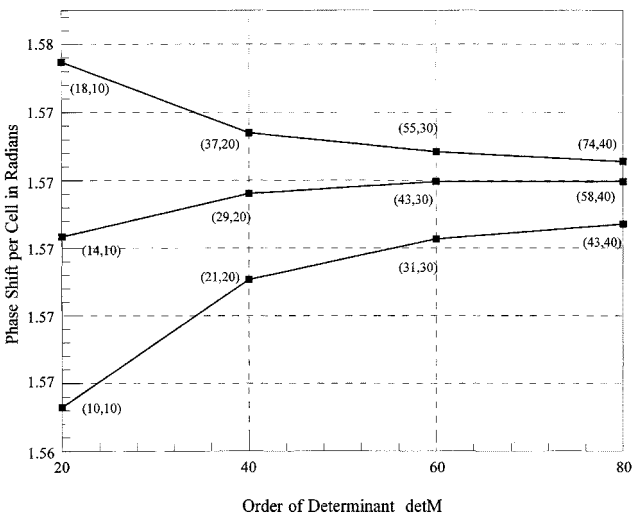

Fig. 5. Convergence behavior of the phase shift per cell at constant frequency $f = 2622.06$ MHz for various values of M and N. The numbers at points mean (M, N).

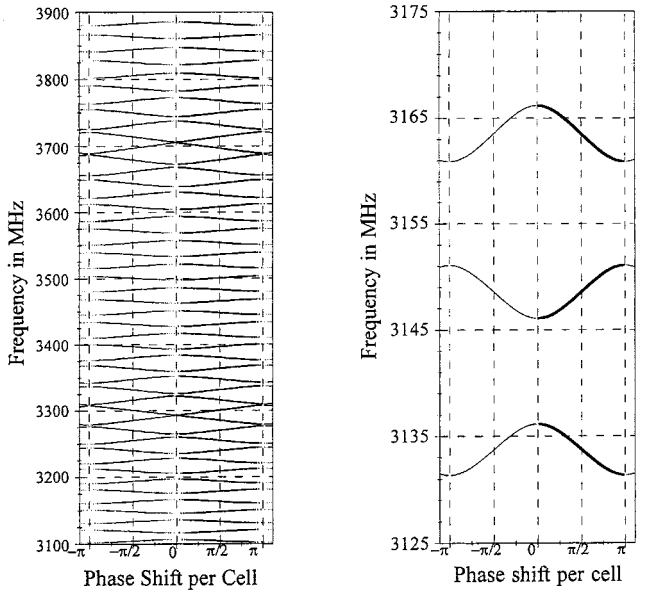

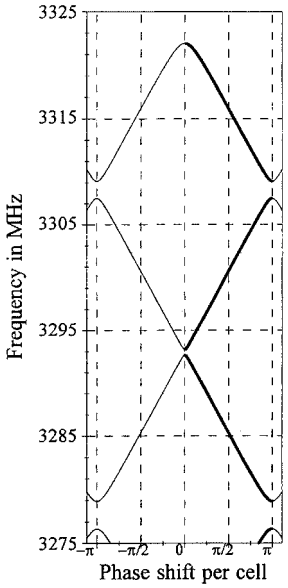

Fig. 6. (a) Section of a dispersion diagram. (b) Detail of narrow-band area. (c) Detail of wide-band area.

VI. Aggregate Dispersion Diagrams

Fig. 5 shows the dependence of the phase shift per cell $\Phi_{M,N}$ on parameters M and N for the same waveguide and frequency as in Section V, i.e., $a^{\mathrm{I}} = 0.0635$ m, $d^{\mathrm{I}} = 0.165$ m, $a^{\mathrm{II}} = 0.044$ m, $d^{\mathrm{II}} = 2.75$ m, $f = 2622.06$ MHz. The pairs of numbers in the parentheses are the parameters (M, N). The correct ratio $M : M = a^{\mathrm{I}} : a^{\mathrm{II}} \simeq 1.4$ is maintained in the middle curve, whereas the upper curve is drawn for the ratio $1.8 > 1.4$ and the lower curve for the ratio $1.0 < 1.4$. The taper-like shape of the curves indicates that, irrespectively of the ratio $M : M$, the curves would approach the asymptotic value Φ with increasing M and N. However, the convergence is much faster for the ratio given by (28). This is consistent with findings of other authors [7], [9], [10]. In the above example, the asymptotic value has been reached already at $\Phi_{43,30} = 1.57296$ rad because a higher choice, i.e., $\Phi_{58,40}$, gave an identical numerical result, i.e., $\Phi_{58,40} = 1.57296$ rad.

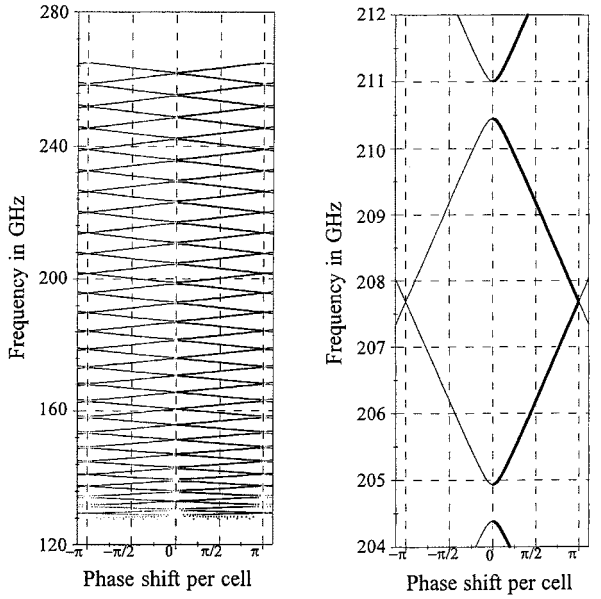

Fig. 7. (a) Section of a dispersion diagram. (b) Detail of an area in Fig. 7(a). The stopband at π mode at 207.675 GHz is only 13-MHz wide, whereas the neighboring passbands are about 2500-MHz wide.

Keeping the choice $(M, N) = (43, 30)$, we can evaluate the whole aggregate dispersion diagram in the allowed frequency region of 2607.76 MHz $< f <$ 3887.59 MHz. It consists of 111 passbands, i.e., dispersion curves. Fig. 6(a) shows a section of the aggregate dispersion diagram starting at 3100 MHz. Notice the smooth modulation in the passband–stopband bandwidths. The bandwidths increase with frequency and reach maximum at $\Delta f = 3307.46$ MHz (πmode)–3293.20 MHz (zero mode) $= 14.26$ MHz. The narrowest stopband is $\Delta f = 3293.198$ MHz (zero mode)–3292.647 MHz (zero mode) $= 0.551$ MHz. As the frequency increases further, the passband width decreases, reaching the minimum at $\Delta f = 3503.457$ MHz (π mode)–3497.801 MHz (zero mode) $= 5.656$ MHz, and the stopband width reaches maximum at $\Delta f = 3515.507$ MHz (π mode)–3503.457 MHz (π mode) $= 12.05$ MHz. The next passband width maximum is at $\Delta f = 3704.810$ MHz (π mode)–3688.794 MHz (zero mode) $= 16.016$ MHz and it is about 400 MHz apart from the previous maximum. The character of dispersion curves changes too. The narrow passband curves have a sine-like shape, whereas the wide passband curves are practically straight lines, except in the neighborhoods of the zero and π modes. The narrow passband and the wide passband areas zoomed are shown in Fig. 6(b) and (c), respectively. The character of the bandwidth modulation in the aggregate depends on the dimensions of the structure.

As the second example, we consider a model of a "multichannel communication line." It is a hollow cylindrical copper conductor, a copper tubing, with the outside diameter of 3 mm. The inside diameter changes stepwise between 2 and 1.8 mm every 20 mm: $a^{\mathrm{I}} = 1$ mm, $a^{\mathrm{II}} = 0.9$ mm,

and $d^{\mathrm{I}} = d^{\mathrm{II}} = 10$ mm. The structure is shallow and the frequency range in which the presented theory is valid is $127.494\ \mathrm{GHz} < f < 262.305\ \mathrm{GHz}$. A section of the aggregate dispersion diagram is shown in Fig. 7(a). Fig. 7(b) shows a part of the diagram zoomed. The bandwidth modulation is less pronounced than in the previous example. The dispersion curves are quite linear, with the exception of the neighborhoods of the zero and π modes. We have approximately $\Phi(f) = \beta_0 L \simeq A + Tf$ or $\omega = 2\pi f \simeq 2\pi\beta_0 L/T - 2\pi A/T$ with some constants A and T. The group velocity v_g of the signal within a channel is then practically independent of frequency: $v_g = (\partial\omega/\partial\beta_0) \simeq (2\pi L/T) = \mathrm{const}$. This means that a signal with a bandwidth within a channel, propagating along the line, will not disperse.

VII. Conclusion

For long cell waveguide structures with stepwise constant circular cross section, the subdivision by transverse matching planes is the most economical one. In this way, the area of the matching planes represents only a small fraction of the entire waveguide boundary. It also naturally creates a chain of cylindrical cavities coupled by two-dimensional (i.e., infinitely thin) coupling elements—the discontinuities themselves.

The theory presented in this paper allows one to evaluate the phase shift per cell of induced TM_0 modes by an explicit formula in long cell periodic structures in a frequency region restricted to the first propagating mode in subregion I. Extension of the frequency range by including the second propagating mode in subregion I would lead to a submatrix of (15), containing the phase shift per cell Φ of no more then the fourth order. Thus, the algebraic resolution of (14) would, in principle, still be possible.

References

[1] R. M. Bevensee, *Electromagnetic Slow Wave Systems*. New York: Wiley, 1964.

[2] R. L. Gluckstern, "Longitudinal coupling impedance in a periodically loaded guide above cut off," in *Proc. ISABELLE Workshop*, May–Aug. 1976.

[3] S. Giordano and J. Votruba, "A method of measuring and calculating microwave coupling impedance of ISABELLE," *IEEE Trans. Nucl. Sci.*, vol. 28, no. 3, p. 2534, 1981.

[4] R. Ryne, Ed., *AIP Conference Proceedings 297, Computational Accelerator Physics*. New York: Amer. Inst. Phys., 1993.

[5] S. Amari, R. Vahldieck, and J. Bornemann, "Complete spectrum of multidepth corrugated waveguides from classical matrix eigenvalues," *IEEE Microwave Guided Wave Lett.*, vol. 9, pp. 7–9, Jan. 1999.

[6] ——, "Analysis of propagation in periodically loaded circular waveguides," *Proc. Inst. Elect. Eng.*, vol. 146, pp. 50–54, Feb. 1999.

[7] S. W. Lee, W. R. Jones, and J. J. Campbell, "Convergence in numerical solutions of iris-type discontinuity problems," *IEEE Trans. Microwave Theory Tech.*, vol. MTT-19, pp. 528–536, June 1971.

[8] J. Esteban and J. M. Rebollar, "Characterization of corrugated waveguides by modal analysis," *IEEE Trans. Microwave Theory Tech.*, vol. 39, pp. 937–943, June 1991.

[9] H. Hahn, C. I. Goldstein, and W. Bauer, "On the theory of iris loaded waveguides," *AEÜ*, vol. 30, pp. 297–302, 1976.

[10] H. Hahn, "On the analysis of periodic waveguide discontinuities by modal field matching," *AEÜ*, vol. 32, pp. 81–85, 1978.

Jan Votruba (M'98) received the Ing. (M.Sc.) degree in technical and nuclear physics from the Czech Technical University, Prague, Czech Republic, in 1961, and the C.Sc. (Ph.D.) degree in theoretical physics from the Czech Academy of Sciences, Prague, Czech Republic, in 1968.

He has held scientific positions at the Institute of Physics, Prague, Czech Republic, the Institut für Experimentelle Kernphysik des Kernforschungszentrums Karlsruhe, Karlsruhe, Germany, and the Brookhaven National Laboratory, Upton, NY. He is currently the Director of RF Technology at the Fonar Corporation, Melville, NY, where he is involved with the 10–30-MHz RF range. He is also with Votruba & Cummings, Melville, NY. His work in periodic structures has been performed privately.